

## An integrated ocean circulation, wave, atmosphere, and marine ecosystem prediction system for the South Atlantic Bight and Gulf of Mexico

Zuo Xue, Joseph Zambon, Zhigang Yao, Yuchuan Liu and Ruoying He\*

Department of Marine, Earth & Atmospheric Sciences, North Carolina State University, Raleigh, NC 27695, USA

An integrated nowcast/forecast modelling system covering the South Atlantic Bight and Gulf of Mexico (SABGOM) is in operation, utilizing sophisticated model coupling and parallel computing techniques. This three-dimensional, high-resolution, regional nowcast/forecast system provides a nowcast and an 84 h forecast of marine weather, ocean waves and circulation, and basic marine ecosystem conditions to the public via a Google Map interface. The SABGOM system runs automatically daily and supports a series of user-defined online applications. Extensive model validations were performed online against in situ and satellite-observed ocean conditions. The SABGOM system exhibits a reliable capability of providing valuable forecasts.

### Introduction

The Gulf of Mexico is a semi-enclosed sea with the maximum depth around 4000 m. It opens to the Caribbean Sea through the Yucatan Strait and to the Atlantic Ocean through the Straits of Florida. The continental shelf of the Gulf of Mexico is broadest along the west coast of Florida. The narrowest portions are along the east coast of Mexico and south of the Mississippi River delta. Several major North American rivers flow into the Gulf of Mexico, the largest of which is the Mississippi River.

The Loop Current and its rings affect, directly or indirectly, almost every aspect of oceanography in the Gulf (Oey et al. 2005). The Loop Current originates at the Yucatan Channel, through which approximately 23–27 Sv ( $1 \text{ Sv} = 10^6 \text{ m}^3/\text{s}$ ) transport passes (Johns et al. 2002; Sheinbaum et al. 2002). The Loop episodically sheds warm-core rings (Vukovich et al. 1979) at intervals of approximately 3–18 months (Sturges & Leben 2000). Tides are generally weak in the Gulf, but strong tropical and extratropical storms often pass through the region, acting as strong synoptic forcing agents for water transport, mixing, and entrainment in the regional ocean (Shay & Uhlhorn 2008).

Downstream of the Gulf of Mexico, the South Atlantic Bight is characterized by a relatively narrow shelf (50–120 km) with a water depth of about 50 m, bounded by the US coast on the west and the Gulf Stream on the east. South of the topographic feature known as the Charleston Bump (at 32°N), the Gulf Stream flows in about 400–600 m of water, with currents of 1 m/s. The Stream is deflected

eastward by the Bump, returns to the shelf edge near 33.5° N, then continues along the shelfbreak to Cape Hatteras (Bane & Dewar 1988). Mesoscale variability is primarily produced by the frontal waves and eddies of the Gulf Stream at the outer edge of the shelf, often accompanied by strong upwelling that can significantly influence biological and chemical distributions on the shelf (Lee et al. 1991; Castelao & He 2013). In the shallowest part of the shelf, there is often a baroclinic southward current associated with a layer of fresh river water (Blanton et al. 1989). The tides (predominantly  $M_2$ ) have a range of 1–3 m along the coast, with tidal excursions of 4–20 km in the inner shelf off South Carolina and Georgia (Blanton et al. 2004). Wind-driven currents lead to strong motions at 5–10-day periods. As in the Gulf of Mexico, a strong variability can be induced by synoptic weather systems (hurricanes and northeasters) moving through the area (Nelson et al. 1999; Blanton et al. 2013). Sea breeze contributes significantly to currents nearshore.

Ever-increasing human activities, such as shoreline development, changes in land use practices, and the resulting increases in pollutant and nutrient/carbon input, continue to threaten the well-being of marine environment and ecosystems in the Gulf of Mexico and South Atlantic Bight waters. Notable results of these impacts are coastal eutrophication, recurring hypoxia [aka the ‘Dead Zone’ (Rabalais et al. 2002)], and coastal ocean acidification (Cai et al. 2011) on the Louisiana-Texas shelf. The coastal regions of the South Atlantic Bight and Gulf of Mexico (SABGOM) are also periodically threatened by

\*Corresponding author. Email: [rhe@ncsu.edu](mailto:rhe@ncsu.edu)

surges induced by storms, which have exhibited a statistically significant trend of increasing in their frequency over the past 90 years (Grinsted et al. 2013).

With rapid advancements in numerical modelling, predicting the above-mentioned marine environment changes and variability is possible. Several global weather [e.g. NCEP, 2.5° resolution (Kalnay et al. 1996)], wave [e.g. Wavewatch III, 2.5° resolution (Tolman 2002)], and ocean (e.g. HYCOM, 1/12° equatorial resolution Chassignet et al. 2007) forecast systems have been operating over the past 10 years. However, the horizontal resolution of some of these forecast systems (e.g. NCEP and Wavewatch III) is too coarse to resolve the variability of ocean conditions on a regional scale, and none of them has realistic river input and ecosystem components. For this reason, we have implemented a high-resolution regional nowcast/forecast system covering the South Atlantic Bight and Gulf of Mexico waters (Figure 1). The SABGOM system incorporates three state-of-the-science modelling components: ROMS (Regional Ocean Modelling System (Shchepetkin & McWilliams 2005, 2009; Haidvogel et al. 2008) for circulation, WRF [Weather Research and Forecasting Model (Skamarock et al. 2005)] for regional atmospheric

circulation, and SWAN [Simulating Waves Nearshore (Booij et al. 1999)] for surface waves. Additionally, the SABGOM system includes an ecosystem modelling component (Fennel et al. 2006, 2011) as a part of the ROMS model. In the following, the interface and functionalities of the nowcast/forecast system are presented first, followed by a detailed description regarding system setup and model validation, and a discussion of model ensembles and future improvements.

### System interface and functionality

To facilitate easy access for users, results of the SABGOM system are broadcasted online via a Google Map interface at <http://omgsrv1.meas.ncsu.edu:8080/ocean-circulation/>. This web interface hosts maps of key predicted variables of marine weather (i.e. 10 m wind, 2 m air temperature, and sea-level pressure), ocean waves (i.e. significant wave height and direction), and ocean circulation (i.e. sea level, three-dimensional temperature, salinity, and current velocity). We also included several model simulated marine ecosystem variables (i.e. concentrations of chlorophyll, phytoplankton, and zooplankton). At this stage, our

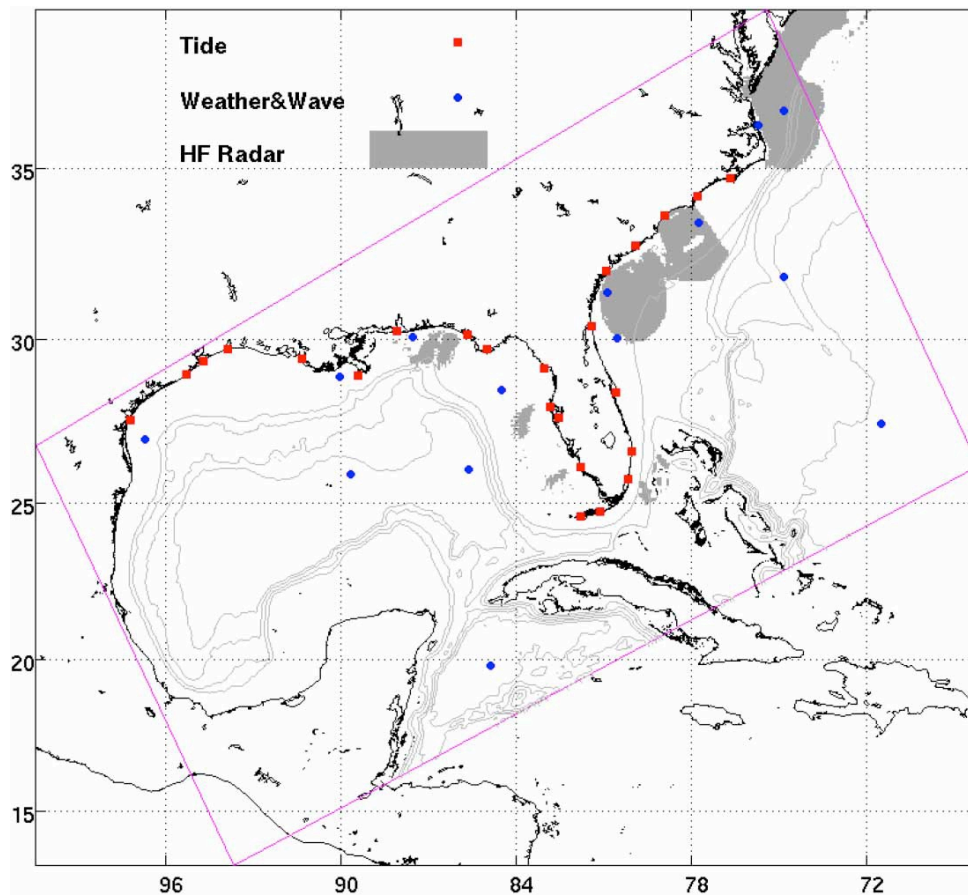


Figure 1. Regional map with water depth (light grey lines), the SABGOM ROMS model domain (pink line), and positions of HF radar and buoys (red and blue dots).

system does not have a watershed model to predict terrestrial input into the ocean, so the fidelity of these marine ecosystem states is constrained by the long-term mean river nutrient concentration and freshwater flux used in the forecast. All forecasted variables are mapped and archived with a 3 h interval. Figure 2 shows screenshots of forecasted 10 m wind, significant wave height, sea surface temperature, and sea surface salinity. On 16 November 2013, the Gulf of Mexico was dominated by a northwestward surface wind moving from the Louisiana coast to the west Florida Shelf [Figure 2(a)]. Associated surface waves were strongest in the open waters southeast off the Mississippi River delta [Figure 2(b)]. Also shown is the low salinity plume from the Mississippi River [Figure 2(c)] as well as the warm water transported by the Loop Current through the Yucatan Strait [Figure 2(d)]. In addition to freshwater input, SABGOM also incorporates riverine nutrient input. On 7 June 2013, high nutrient concentration was forecasted around the Mississippi/Atchafalaya river mouth owing to enormous terrestrial input [Figure 3(a)], which led to extensive primary production as shown by high concentration

chlorophyll, and abundant phytoplankton, and zooplankton in the adjacent coastal waters [Figure 3(b)-(d); see (Xue et al. 2013) for details of the SABGOM's ecosystem model].

SABGOM's web interface also supports online user-defined functions such as sampling vertical profiling, transects, and 84 h particle trajectory prediction at any user-defined time and location within the SABGOM domain. Users can select their desired date, location, and variables and the system will extract, plot, and display corresponding vertical profiles [Figure 4(a)] or cross-sections of temperature, salinity, and current velocity [Figure 4(b)]. In addition, users can release a number of surface floats or particles by either clicking on the map or manually inputting longitudes and latitudes. The SABGOM system will calculate based on the fourth-order Runge-Kutta method and plot the forecasted trajectory of these floats for the next 84 h [Figure 4(c)]. Further, the web interface also has information for model validation against various observations, model ensembles, and other useful data links, which will be described in later sections. The SABGOM model digital outputs are also available for download at the following

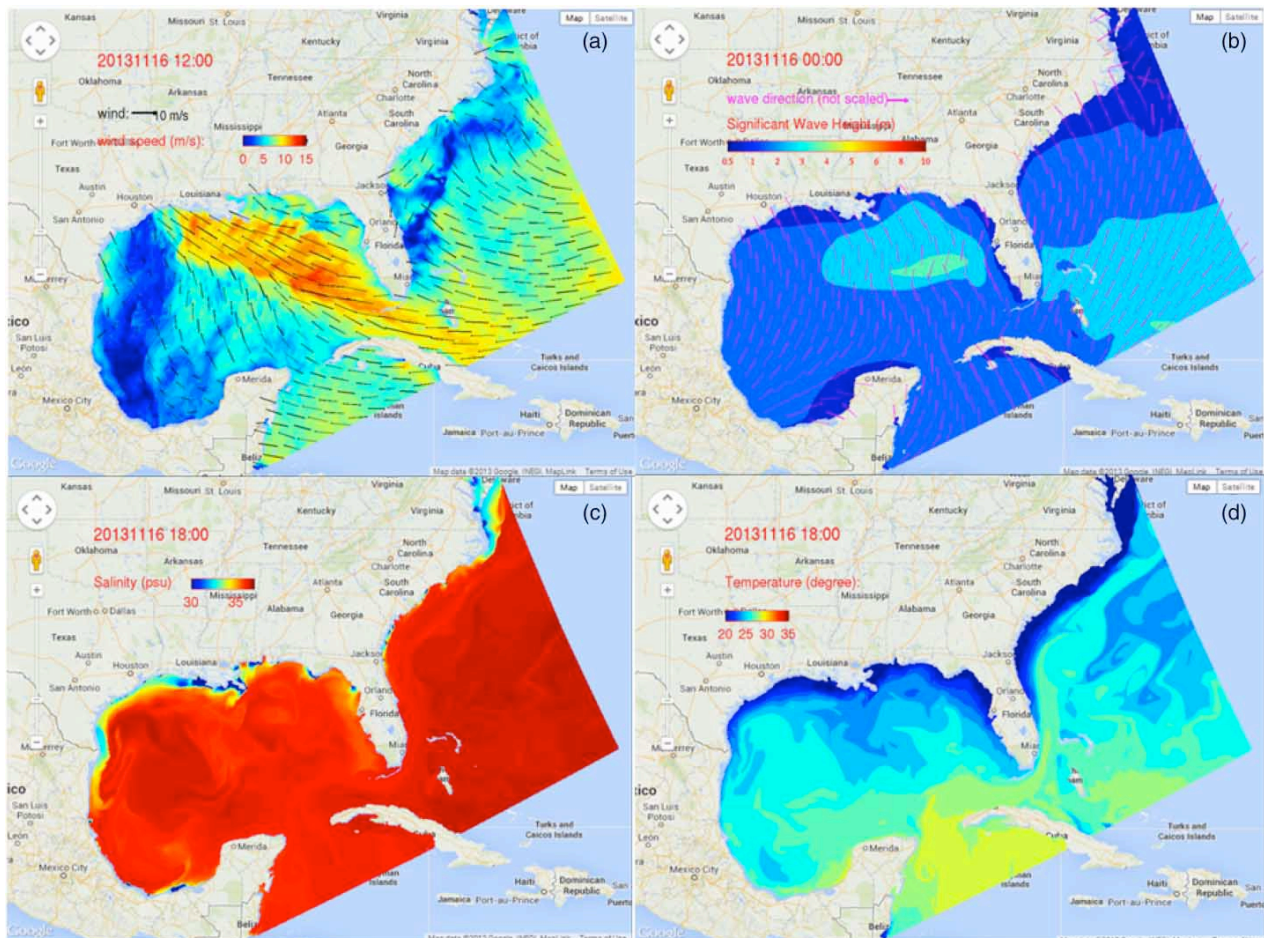


Figure 2. Screenshots of the SABGOM web interface showing (a) surface wind, (b) significant wave height, (c) sea surface salinity, and (d) sea surface temperature at different times on 16 November 2013.

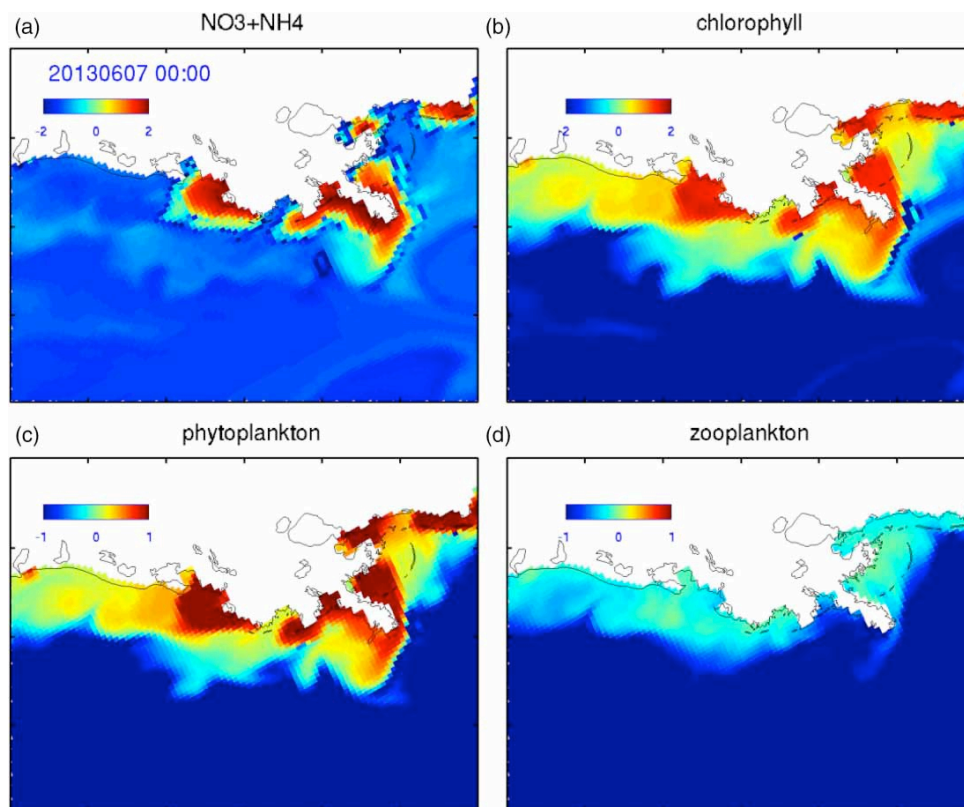


Figure 3. Close examination of SABGOM-forecasted ecosystem condition in the Louisiana Shelf on 7 June 2013. (a) Nutrients, (b) chlorophyll, (c) phytoplankton, and (d) zooplankton (colour maps are in log scale, unit:  $\text{mg N/m}^3$ ).

THREDDS server: <http://omgsrv1.meas.ncsu.edu:8080/thredds/dodsC/fmrc/sabgom/>.

## Model setup and validations

### Model setup

#### Ocean model (ROMS)

The circulation nowcast/forecast model was implemented based on the ROMS. The model domain (Figure 1) encompasses the entire Gulf of Mexico and South Atlantic Bight. Details of our ocean model implementation see (Hyun & He 2010; Xue et al. 2013). Briefly, the model has a horizontal resolution of 5 km. Vertically, there are 36 terrain-following layers weighted to better resolve surface and bottom boundary layers. For open boundary conditions, the ocean model is one-way nested inside the  $1/12^\circ$  data assimilative North Atlantic Hybrid Coordinate Ocean Model [HYCOM/NCODA (Chassignet et al. 2007)]. At the model's open boundaries, free surface and depth-averaged velocity were specified using the external subtidal information defined by HYCOM/NCODA superimposed by eight tidal constituents ( $Q_1$ ,  $O_1$ ,  $P_1$ ,  $K_1$ ,  $N_2$ ,  $M_2$ ,  $S_2$ , and  $K_2$ ) derived from the OTIS regional tidal solution (Flather, 1976; Egbert & Erofeeva 2002). No equilibrium tides are included in the current set up. The 3-hourly, 32 km horizontal resolution

NOAA NCEP reanalysis or forecast (<http://www.esrl.noaa.gov/psd/>) was utilized for both meteorological momentum and buoyancy forcing. A 180 s time step was used for iterations, and the model output was every 3 h.

The ocean circulation model was coupled with a marine biogeochemical model described in references 25 and 26. A 7-year model hindcast (2004–2010) was performed and validated against satellite-observed sea surface height and surface chlorophyll, and in situ observations including coastal sea level, ocean temperature, salinity, and dissolved inorganic nitrogen concentrations (Xue et al. 2013).

Unlike the hindcast parameters, there is no real-time nutrient measurement from rivers. The nowcast/forecast system utilizes monthly mean climatology based on river conditions during 2004–2010 (Xue et al. 2013). The initial and boundary conditions of the biological variables are from model-forecast conditions of the previous cycle. That is, every day the biological prediction is initialized using the nowcast condition provided by the previous nowcast/forecast cycle.

#### Atmospheric model (WRF)

The atmosphere nowcast/forecast model was implemented based on WRF using the Advanced Research WRF (ARW) dynamical core. Details of this model implementation are

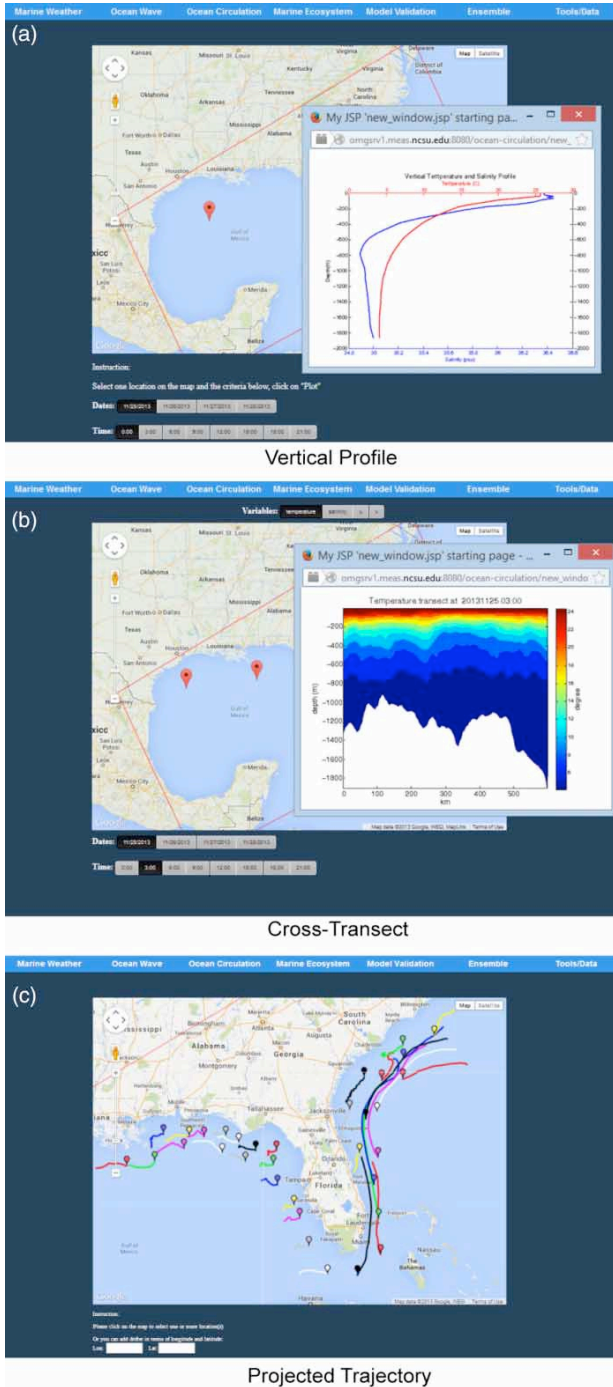


Figure 4. Screenshots of user-defined inquiries of (a) vertical profile (temperature and salinity as of 00Z 25 November 2013), (b) cross-section (temperature fields as of 03Z 25 November 2013; red balloon indicates the location of the vertical profile/cross-transect), and (c) an 84 h surface trajectory forecast (as of 00Z 25 November 2013; coloured balloons indicate the initial release points and coloured lines indicate forecasted trajectories over the next 84 h).

given in reference 31. Briefly, the model initial and boundary conditions were derived from daily Global Forecast System (GFS) output (00Z forecast) with a horizontal

grid spacing of  $0.5^\circ$  (available online: <http://nomads.ncep.noaa.gov/pub/data/nccf/com/gfs/prod/>). These data are interpolated onto a 7–9 km horizontal grid covering the entire US east coast, with 31 vertical levels for the initial condition. A 30 s time step is used for iteration, and the simulation output was made every 3 h. Grid-resolved precipitation is computed using the WRF Single-Moment 6-class microphysics scheme (WSM-6) (Hong & Lim 2006). This first-order microphysics scheme features water vapor, cloud water, cloud ice, rain, snow, and graupel. The Kain–Fritsch CP scheme (Kain 2004) is used to parameterize precipitation processes on a sub-grid scale. Longwave and shortwave radiation physics are computed using the Rapid Radiative Transfer Model (RRTM) (Dudhia 1989; Mlawer et al. 1997), called every 15 min. The Eta surface layer scheme (Janjic 1996, 2002) based on similarity theory (Monin & Obukhov 1954) physics option is used along with the Noah land surface model (Chen & Dudhia 2001). Finally, the Mellor–Yamada–Janjic turbulent kinetic energy planetary boundary layer (PBL) model (Janjic 1990, 1996, 2002; Mellor & Yamada 1982) is called every time step on both WRF domains.

#### Wave model (SWAN)

The surface wave nowcast/forecast model was implemented based on SWAN, which is a spectral wave model that solves the spectral density evolution equation (Booij et al. 1999). The SWAN model has the same spatial coverage as the WRF model (details of SWAN implementation see reference Zamboni et al.). To provide surface forcing for the wave model, 10 m winds are utilized from the GFS model with an interval of 3 h. Initial conditions are generated by running the model for several iterations with GFS winds at the initial time in ‘Stationary Mode’ until the solutions converged. In our SWAN setup, directional space is utilized with 36 directional bins and 24 frequency bins of 1 s width between 1 s and 25 s. Non-linear quadruplet wave interactions are activated in the model. Wave bottom dissipation is parameterized using the formulation in reference (Madsen et al. 1988), with an equivalent roughness length scale of 0.05 m. The depth-induced breaking constant, e.g. the wave height-to-water depth ratio for breaking waves, is set to 0.73. Wind-wave growth is generated using the Komen formulation (Komen et al. 1984). A backward-in-space, backward-in-time advection scheme is used for iteration. Following forecast completion, significant wave height, wave direction, and wavelength are output every 3 h.

#### System operation

As previously described, the initial and boundary conditions of the SABGOM rely on several global forecast

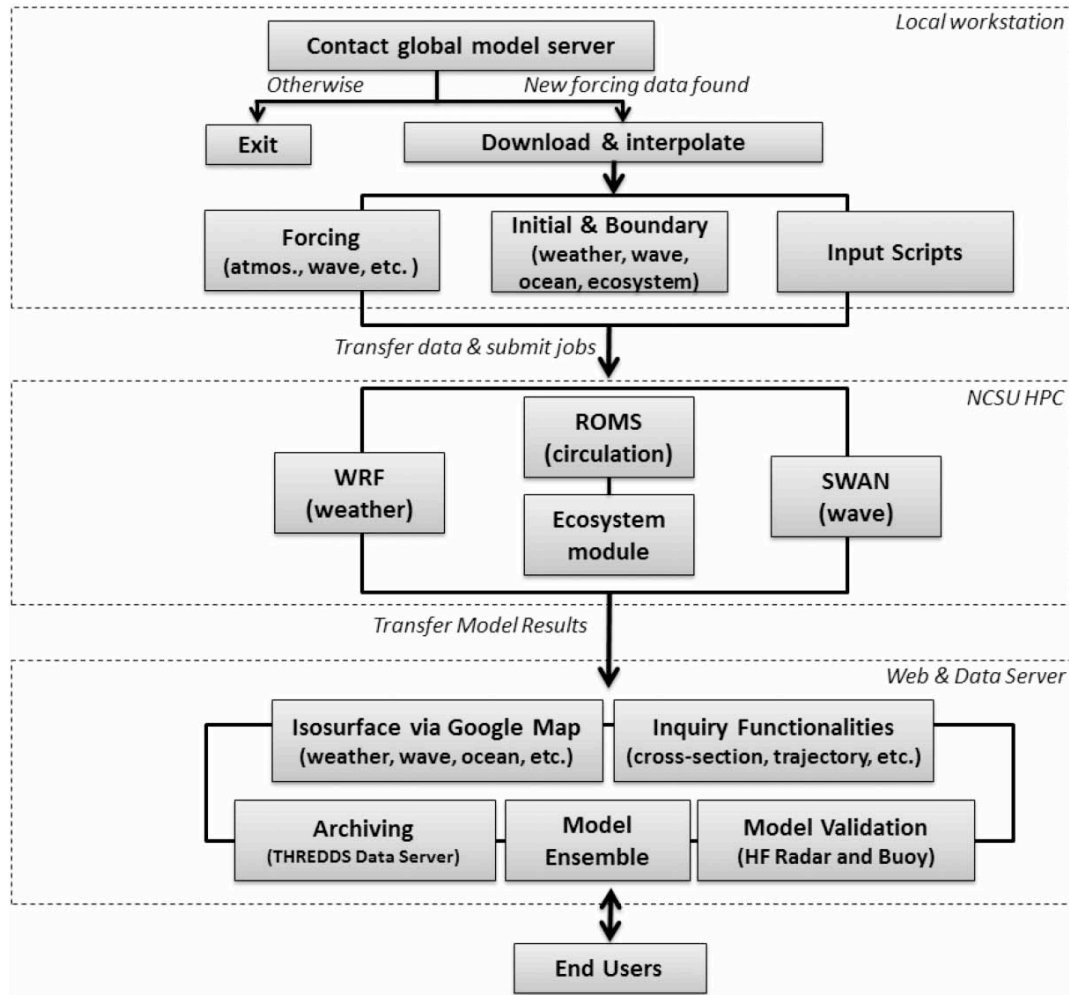


Figure 5. Conceptual flow chart of the SABGOM forecast system.

products (i.e. GFS for weather and wave, NARR and HYCOM/NCODA for ocean), which usually provide an 84 h or even longer forecast on their data servers. Figure 5 shows a flow chart of the SABGOM's daily operation. In our daily operation, SABGOM nowcast and forecast (e.g. time = T) are initialized using the HYCOM solutions at (T- 7 days). The simulation is run for 11 days (7-day spin up, 1-day nowcast, plus 3-day forecast). The nowcast/forecast system is initialized automatically by shell scripts at a local Linux workstation. First, the local workstation contacts global model data servers every 6 h. Once a new solution is available, the workstation downloads the data. The input scripts for corresponding models are also generated. Second, all data, including forcing, initial and boundary conditions, and input scripts are transferred to the High Performance Computing (HPC) system at North Carolina State University, where 112 computing nodes are reserved 24/7 for nowcast/forecast operations. As all three models support parallel computation via the Message Passing Interface, an 84 h

weather, wave, and ocean condition forecast will take less than 4 h using 112 cores (48 for WRF, 32 for SWAN, and 32 for ROMS). Third, upon the completion of all three simulations, model results are transferred back to a local web/data server and archived on the THREDDS server. Meanwhile, maps of selected variables will be automatically generated and linked to the web interface. Model validation against available observations, ocean model ensembles will also be produced online.

#### Model validations

To validate model skills and ensure forecast quality, the SABGOM system is programmed to automatically download observations from National Ocean Service (<http://tidesandcurrents.noaa.gov/>) and National Data Buoy Center (<http://www.ndbc.noaa.gov/>) and generate validation plots on a daily basis. To assess the model's performance over a longer time-scale, SABGOM-forecasted sea level anomaly, sea-level air pressure, and significant

wave height were compared against observations at numerous sites, such as Wrightsville Beach, NC [Station ID: 8658163, Figure 6(a)]; Charleston, SC [Station ID: 8665530, Figure 6(b)]; Naples FL [Station ID: 8725110, Figure 6(c)]; Savannah, GA [Station ID: 41008, Figures 6(d) and (g)]; Southwest Pass, LA [Station ID: 42001, Figure 6(e) and (h)], and West of Naples, FL [Station ID: 42003, Figure 6(f) and (i)]. Over a 1-month period (16 September 2013 to 16 October 2013), model-forecasted sea level, sea-level pressure, and significant wave height time series tracked their observational counterparts reasonably well at all stations. The correlation coefficient (R) between forecasted and observed fields was more than 0.9, except for the sea-level and wave forecast at West of Naples, FL (R = 0.89 and 0.72). In addition, SABGOM is capable of forecasting synoptic surge events [e.g. wave height > 2.0 m, shown in Figure 6(g) and (h)]. A more robust statistical assessment of the model's forecast skill is shown in the form of a Taylor diagram (Taylor 2001) (Figure 7), where correlation coefficients, centred root mean square differences between observed and model-forecasted sea levels, sea-level pressure, and wave height, and their normalized standard deviations, are all presented in a single plot. At most of the coastal stations covered by the SABGOM, these correlation coefficients

ranged between 0.70 and 0.98, and the forecasted variables are within one standard deviation of their observed counterparts.

In addition to comparing with point measurements, the SABGOM system downloads 2-D surface current fields observed by High Frequency Radars along the coast (data can be downloaded from the Coastal Observing Research and Development Center, <http://cordc.ucsd.edu/mapping/>) and provides side-by-side comparisons between observed and forecasted surface current within the radar footprints at 3 h intervals. As an example, Figure 8 shows the surface current fields observed by HF radar and model-forecasted fields off Charleston, SC [Figure 8(a) and (b)]; Savannah, GA [Figure 8(c) and (d)]; and Miami, FL [Figures 8(e) and (f)]. At all three areas, forecasted surface currents generally agree with observations in both direction and speed. Compared with HF Radar's limited spatial coverage, SABGOM provides a more comprehensive regional circulation pattern in a larger spatial context.

Satellite-observed ocean surface conditions were also used for validating SABGOM's performance over the entire model domain. Figure 9, for example, is a snapshot of satellite-observed sea surface height [Figure 9(a)] wind speed [Figure 9(b)], and significant wave height [Figure 9(c)] (spatial resolution is  $0.2^\circ \times 0.3^\circ$  for sea surface

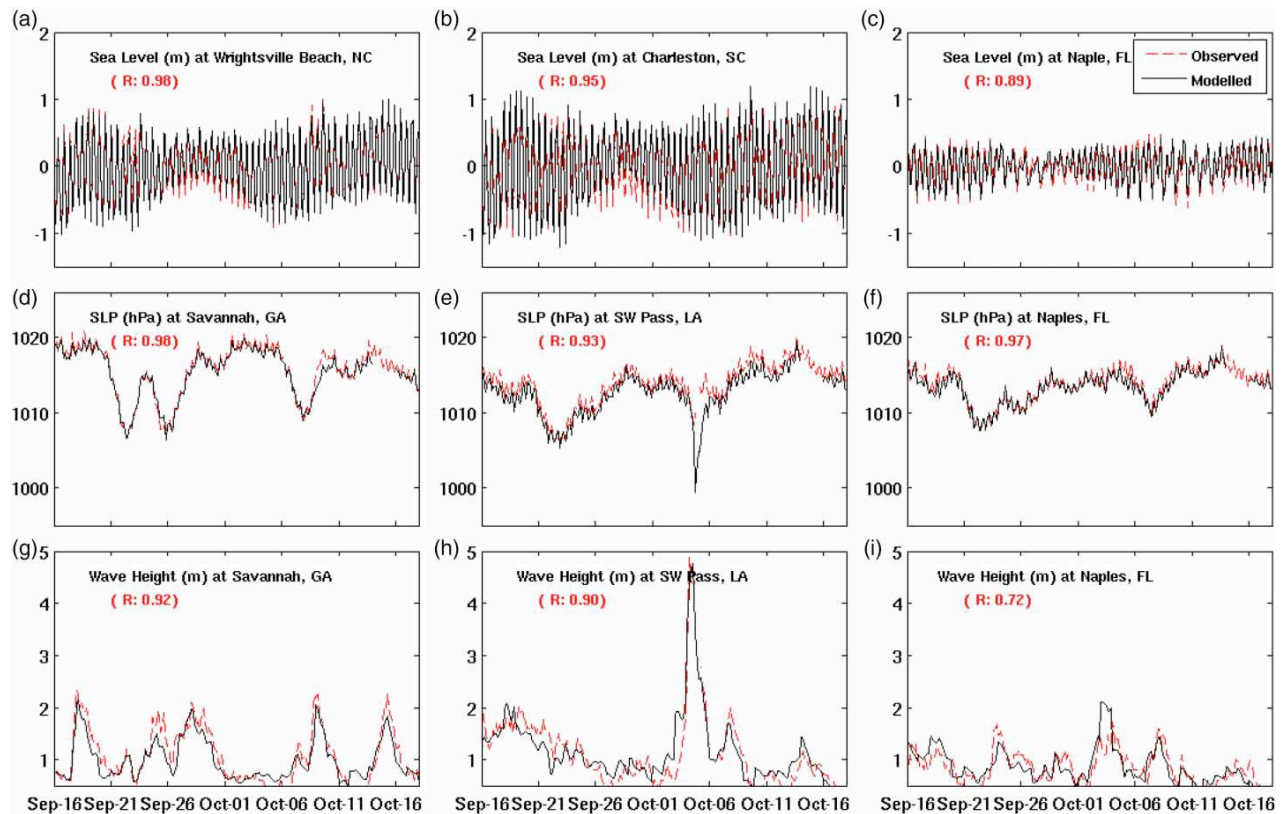


Figure 6. Time series of forecasted (black solid line) and observed (red dashed line) sea level anomalies at (a) Wrightsville Beach, NC, (b) Charleston, SC and (c) Naples, FL; sea-level pressure at (d) Savannah, GA (e) SW Pass, LA and (f) Naples, FL; and significant wave height at (g) Savannah, GA, (h) Southwest Pass, LA and (i) Naples, FL from 16 September 2013 to 16 October 2013.

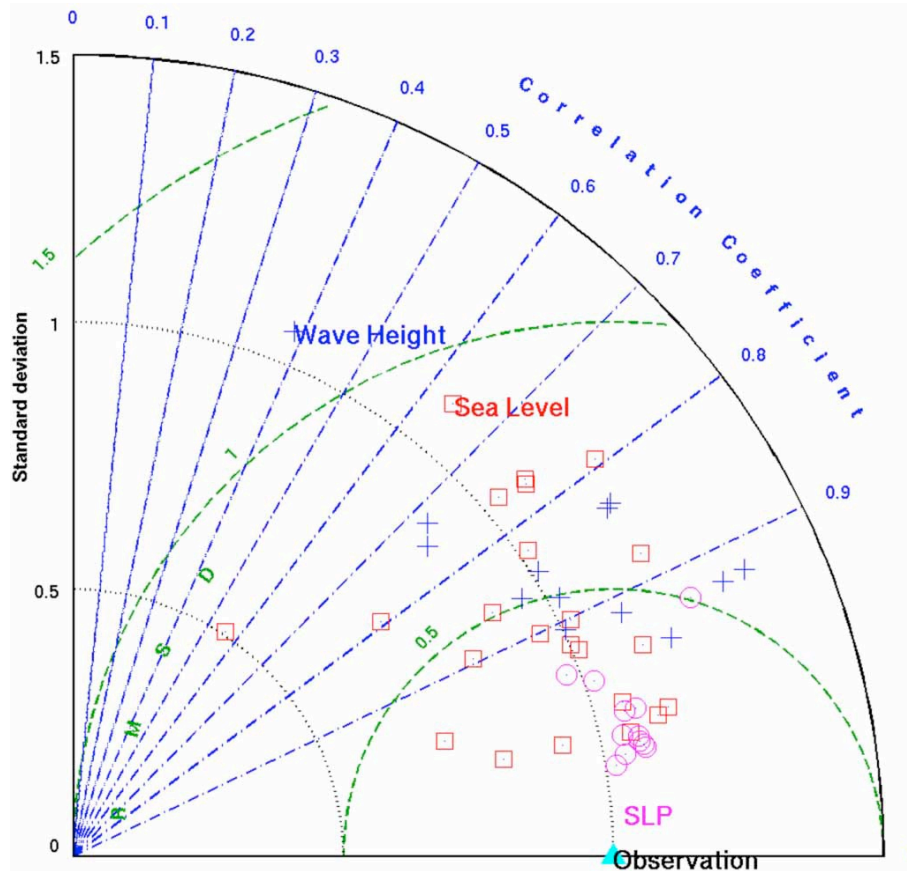


Figure 7. Taylor diagram for statistics of SABGOM-forecasted and observed sea level anomalies (pink circles), sea-level pressure (green squares), and significant wave height (blue crosses) at buoys within the model domain. Radial distance represents the ratio of forecasted to observed standard deviations, and azimuthal angle represents forecast-observation correlation. Green arcs represent centred root mean square difference between forecast and observation.

height,  $0.25^\circ$  for wind, and  $1^\circ$  for wave; data product are generated by Ssalto/Duacs and distributed by Aviso, <http://www.aviso.oceanobs.com/duacs/>) and their SABGOM-forecasted counterparts [Figure 9(d)–(f)] on 27 September 2013. The SABGOM system reproduced these surface ocean conditions, such as the high (warm) water levels associated with the Loop Current around the Yucatan Shelf, a warm core eddy in the centre of the Gulf of Mexico [Figure 9(a) and (d)], and the strong wind [Figure 9(b) and (e)] and associated high waves [Figure 9(c) and (f)] conditions in the South Atlantic Bight. SABGOM over-estimated wind speed in the Gulf of Mexico and wave strength in the Sargasso Sea. Such a mismatch may be attributed to the coarse resolution of the global model (i.e. GFS), by which the wave model is forced.

## Discussion

### Model ensembles

Considering the uncertainty associated with different models, the use of model ensembles can be an effective

means of tracking individual model errors, thus forming more reliable predictions of coastal ocean conditions (Lermusiaux et al. 2006). On a daily basis, the solution of the SABGOM was compared against two global HYCOM products: the NOAA global operational Real-Time Ocean Forecast System (RTOFS) and the Navy global HYCOM/NCODA. Compared with global models, SABGOM has several advantages, including (1) a relatively high horizontal resolution, which enables a better representation of coastal geometry and ocean bathymetry; (2) incorporation of tides and riverine inputs as boundary conditions, which can improve forecast accuracy of sea-level variations, vertical mixing, and river plume dynamics; (3) built-in ecosystem and sediment modelling components (Warner et al. 2008; Fennel et al. 2006, 2011), which are crucial for addressing marine environmental issues; and (4) support of model nesting and coupling with other physical models [e.g. WRF and SWAN (Warner et al. 2010)].

Figure 10 shows the surface currents in the northern Gulf of Mexico forecasted by SABGOM, HYCOM/NCODA, RTOFS, and the ensemble mean of the three solutions on

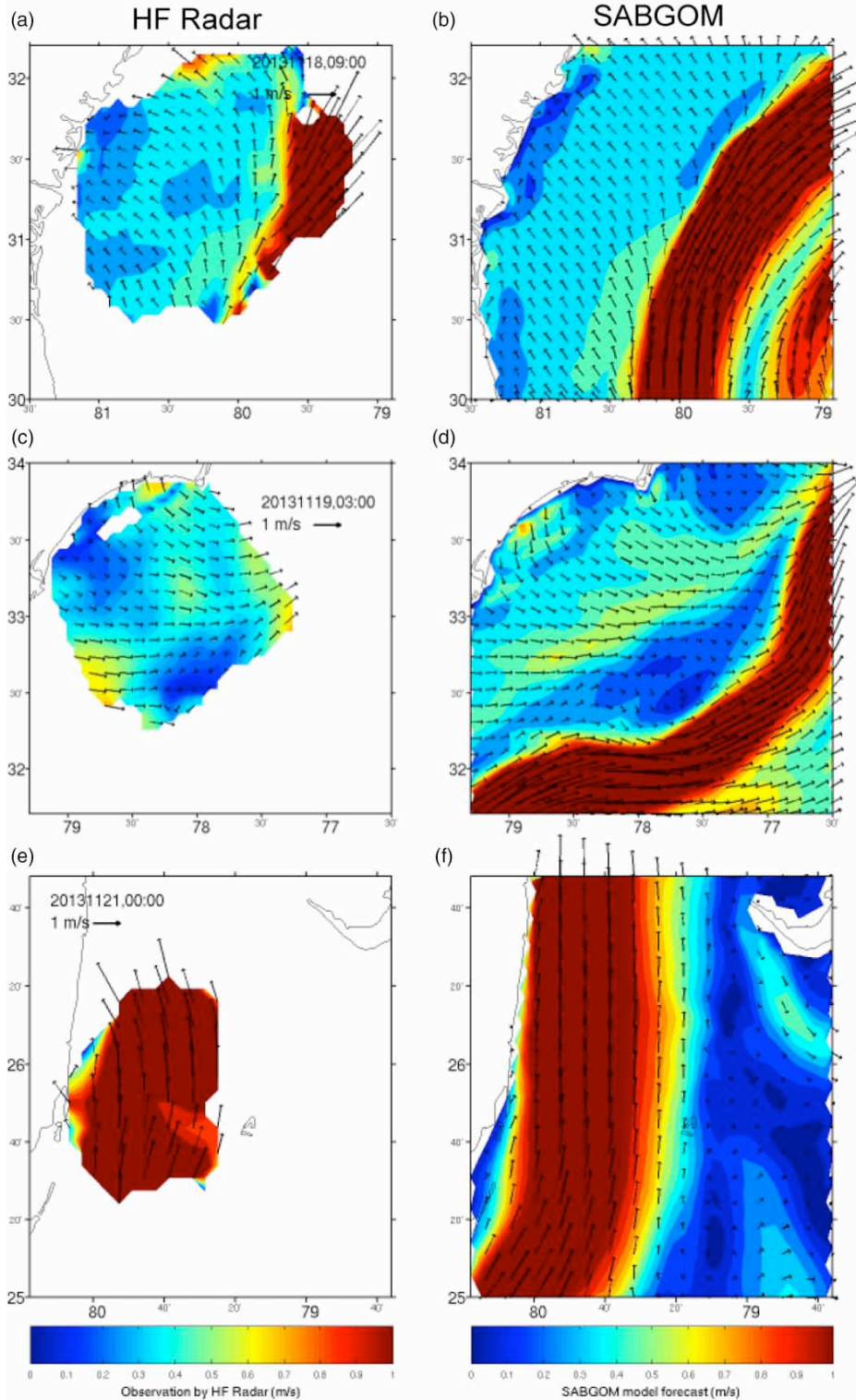


Figure 8. Surface current fields observed by HF Radar (left panels) and forecasted by SABGOM (right panels) at Charleston, SC [(a) and (b)], Savannah, GA [(c) and (d)], and Miami, FL [(e) and (f)].

00Z 7 June 2013. In general, all three models were able to reproduce the Loop Current, which is the dominant circulation feature in the outer shelf and deep ocean. However, a closer examination of the circulation on the inner shelf

reveals significant differences among the three solutions: while the two global forecasts indicate small velocities [Figure 10(b) and (c)], SABGOM forecasted a strong westward transport. Such difference between the SABGOM

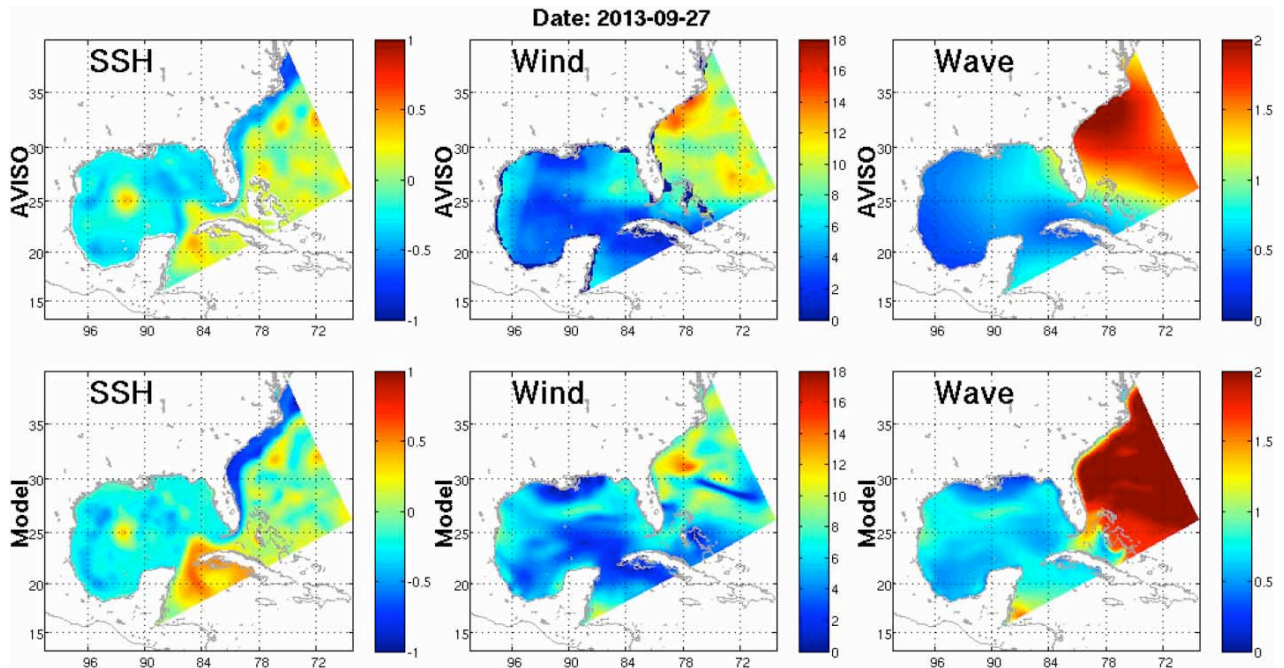


Figure 9. Satellite-observed (AVISO) sea surface height (SSH, a, unit: m), wind speed (b, unit: m/s), and significant wave height (c, unit: m) and their SABGOM-forecasted counterparts [(d), (e), and (f)].

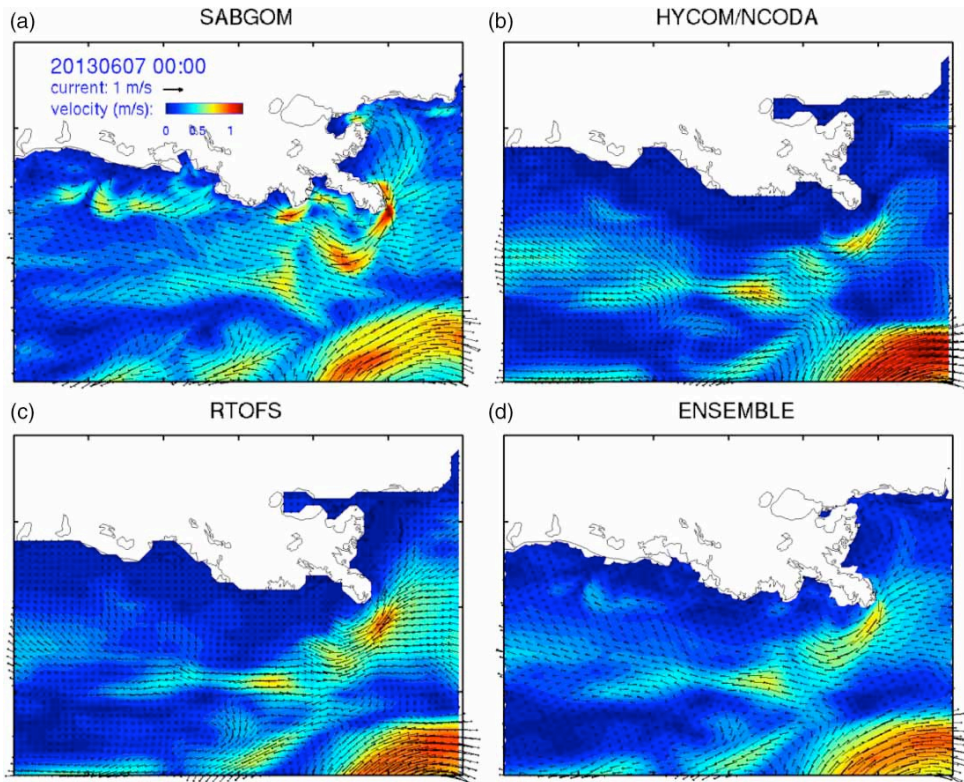


Figure 10. Surface current field as of 00Z 7 June 2013, forecasted by (a) SABGOM, (b) HYCOM/NCODA, (c) RTOFS, and (d) an average of the three solutions.

and global products was ascribed to SABGOM's higher horizontal resolution and bathymetry, as well as its incorporation of tides and freshwater inputs. The three-member ensemble [Figure 10(d)] can be constructed by averaging SABGOM, HYCOM and RTOFS forecasts.

#### Future system refinements

The SABGOM system was originally designed in 2007 and has been evolving since then with continued refinement to improve model performance, new model-data validations, and better information exchange interface. One challenge that emerged during the development of the SABGOM was the treatment of river forcing, which consists of freshwater discharge and associated nutrient flux. While freshwater discharge of major rivers (e.g. Mississippi and Atchafalaya) could be accessed on a near-real-time basis via gauge stations operated by the US Geological Survey, measurement of nutrient concentration is still sporadic at best (two or three measurements per month). As described in the previous section, the SABGOM has to rely on monthly mean climatology for river nutrient input. In addition, because there is no global marine ecosystem model prediction, the specification of boundary conditions of SABGOM's marine ecosystem nowcast/forecast also relies on the result from 2004 to 2010 hindcast (Xue et al. 2013). This, together with a lack of real-time riverine nutrient flux data, renders the SABGOM's ability to accurately predict regional marine ecosystem conditions, an area that has clear need for future improvement.

During the process of SAMGOM system development, an online coupling of the three models (WRF, SWAN, and ROMS) via a model coupler [Model Coupling Toolkit (Jacob et al. 2005; Larson et al. 2005)] was implemented (Warner et al. 2010). Through the dynamical couplings among ocean wave, ocean circulation and atmosphere, important processes such as wave-induced enhancement of surface roughness, energy dissipation and mixing can be better accounted for. Implementation of such a fully coupled modelling system is under way to upgrade SABGOM, and it will further improve SABGOM's ability in nowcasting and forecasting synoptic events such as hurricanes and winter storms (Zambon et al.).

#### Summary

An integrated marine environment nowcast/forecast system for the SABGOM is presented in this study. This high-resolution, regional system consists of three state-of-the-science models: WRF for ocean weather, SWAN for surface waves, and ROMS for ocean circulation. All three models are driven by forecasted fields from global models and operated automatically on a daily basis. The SABGOM system's daily nowcast and 84 h forecast of ocean conditions can be visualized online via a Google

Map interface, which also supports several valuable user-defined online functions, such as sampling vertical profiling, transect, and predicting particle trajectories. Extensive model validations against satellite-observed data and in situ observations are made daily to provide a quality control and assessment of SABGOM in predicting regional coastal ocean conditions. Further improvements in the SABGOM system can take advantage of recent advancements in atmosphere-wave-ocean model coupling, and more observations for validation or assimilation.

#### Acknowledgements

Editorial assistance from J. Warrillow is acknowledged.

#### Disclosure statement

No potential conflict of interest was reported by the authors.

#### Funding

This work was supported by Gulf of Mexico Research Initiative/GISR [grant number 02-S130202]; NOAA [grant number NA11NOS0120033]; NASA [grant numbers NNX10AU06G, NNX12AP84G, and NNX13AD80G].

#### References

- Bane JM, Dewar WK. 1988. Gulf Stream bimodality and variability downstream of the Charleston bump. *J Geophys Res.* 93 (C6):6695–6710.
- Blanton BO, et al. 2004. Barotropic tides in the south Atlantic bight. *J Geophys Res.* 109(C12):C12–024.
- Blanton JO, et al. 1989. Advection of momentum and buoyancy in a coastal frontal zone. *J Phys Ocean.* 19(1):98–115.
- Blanton JO, et al. 2013. Wind stress climatology in the south atlantic bight, in oceanography of the southeastern U.S. continental shelf. *Am Geophy Union.* 10–22, doi:10.1029/CO002p0010.
- Booij N, Ris R, Holthuijsen LH. 1999. A third-generation wave model for coastal regions: 1. Model description and validation. *J Geophys Res.* 104(C4):7649–7666.
- Cai WJ, et al. 2011. Acidification of subsurface coastal waters enhanced by eutrophication. *NatGeosci.* 4(11):766–770.
- Castelao RM, He R. 2013. Mesoscale eddies in the south Atlantic bight. *J Geophys Res.* 118(10):5720–5731.
- Chassignet EP, et al. 2007. The HYCOM (HYbrid Coordinate Ocean Model) data assimilative system. *J Marine Syst.* 65 (1–4):60–83.
- Chen F, Dudhia J. 2001. Coupling an advanced land-surface/hydrology model with the Penn State / NCAR MM5 modeling system. Part I: Model description and implementation. *Mon Weather Rev.* 129:569–585.
- Dudhia J. 1989. Numerical study of convection observed during the winter monsoon experiment using a mesoscale two-dimensional model. *J Atmos Sci.* 46(20):3077–3107.
- Egbert GD, Erofeeva SY. 2002. Efficient inverse modeling of Barotropic ocean tides. *J Atmos Oceanic Technol.* 19 (2):183–204.
- Fennel K, Wilkin J, Levin J, Moisan J, O'Reilly J, Haidvogel D. 2006. Nitrogen cycling in the middle Atlantic bight: results

- from a three-dimensional model and implications for the North Atlantic nitrogen budget. *Global Biogeochem Cycles*. 20:GB3007, doi:10.1029/2005GB002456.
- Fennel K, et al. 2011. A coupled physical-biological model of the Northern Gulf of Mexico shelf: model description, validation and analysis of phytoplankton variability. *Biogeosciences*. 8:1881–1899.
- Flather RA. 1976. A tidal model of the northwest European continental shelf. *Memoires de la Societe Royale de Sciences de Liege*. 6:141–164.
- Grinsted A, Moore JC, Jevrejeva S. 2013. Projected Atlantic hurricane surge threat from rising temperatures. *Proc Nat Acad Sci*. 5369–5373, doi:10.1073/pnas.1209980110.
- Haidvogel DB, et al. 2008. Ocean forecasting in terrain-following coordinates: Formulation and skill assessment of the Regional Ocean Modeling System. *J Comput Phys*. 227(7):3595–3624.
- Hong SY, Lim JOJ. 2006. The WRF single-moment 6–class microphysics scheme (WSM6). *J. Korean Meteor. Soc.* 42(2):129–151.
- Hyun KH, He R. 2010. Coastal upwelling in the South Atlantic Bight: A revisit of the 2003 cold event using long term observations and model hindcast solutions. *J Marine Syst*. 83(1–2):1–13.
- Jacob R, Larson J, Ong E. 2005.  $M \times N$  communication and parallel interpolation in Community Climate System Model Version 3 using the model coupling toolkit. *Int J High Perform Comput Appl*. 19(3):293–307.
- Janjic ZI. 1990. The step-mountain coordinate: physical package. *Mon Weather Rev*. 118:1429–1443.
- Janjic ZI. 1996. The surface layer in the NCEP Eta model. in *Eleventh Conference on Numerical Weather Prediction*. Norfolk, VA: Amer. Meteor. Soc.
- Janjic ZI. 2002. Nonsingular implementation of the Mellor–Yamada Level 2.5 scheme in the NCEP Meso model, in *NCEP Office Note*. p. 61.
- Johns WE, et al. 2002. On the Atlantic inflow to the Caribbean Sea. *Deep Sea Res Part I*. 49(2):211–243.
- Kain JS. 2004. The Kain-Fritsch convective parameterization: an update. *J Appl Meteor*. 43(1):170–181.
- Kalnay E, et al. 1996. The NCEP/NCAR 40–year reanalysis project. *Bull Am Meteor Soc*. 77(3):437–471.
- Komen G, Hasselmann K, Hasselmann K. 1984. On the existence of a fully developed wind-sea spectrum. *J Phys Ocean*. 14(8):1271–1285.
- Larson J, Jacob R, Ong E. 2005. The model coupling toolkit: A new Fortran90 toolkit for building multiphysics parallel coupled models. *Int J High Perform Comput Appl*. 19(3):277–292.
- Lee TN, Yoder JA, Atkinson LP. 1991. Gulf Stream frontal eddy influence on productivity of the southeast U.S. continental shelf. *J Geophys Res*. 96(C12):22191–22205.
- Lermusiaux PF, et al. 2006. Quantifying uncertainties in ocean predictions. DTIC Document.
- Madsen OS, Poon YK, Graber HC. 1988. Spectral wave attenuation by bottom friction: Theory. *Coastal Eng Proc*. 1(21):492–504.
- Mellor GL, Yamada T. 1982. Development of a turbulence closure model for geophysical fluid problems. *Rev Geophys*. 20(4):851–875.
- Mlawer EJ, et al. 1997. Radiative transfer for inhomogeneous atmosphere: RRTM, a validated correlated-k model for the longwave. *J Geophys Res*. 102:16663–16682.
- Monin A, Obukhov A. 1954. Basic laws of turbulent mixing in the surface layer of the atmosphere. *Contrib. Geophys. Inst. Acad. Sci. USSR*. 151:163–187.
- Nelson JR, et al. 1999. Benthic microalgal biomass and irradiance at the sea floor on the continental shelf of the South Atlantic Bight: Spatial and temporal variability and storm effects. *Conti Shelf Res*. 19(4):477–505.
- Oey LY, Ezer T, Lee HC. 2005. Loop current, rings and related circulation in the Gulf of Mexico: A review of numerical models and future challenges, in *circulation in the gulf of Mexico: Observations and models*. Am Geophys Union. 31–56, doi:10.1029/161GM04.
- Rabalais N, Turner RE, Wiseman WJJ. 2002. Gulf of Mexico Hypoxia, A.K.A. the dead zone. *Annu Rev Ecol Syst*. 33:235–263.
- Shay LK, Uhlhorn EW. 2008. Loop current response to hurricanes Isidore and Lili. *Mon Weather Rev*. 136(9):3248–3274.
- Shchepetkin AF, McWilliams JC. 2005. The regional ocean modeling system (ROMS): A split-explicit, free-surface, topography-following coordinates ocean model. *Ocean Model*. 9:347–404.
- Shchepetkin AF, McWilliams JC. 2009. Correction and commentary for “Ocean forecasting in terrain-following coordinates: Formulation and skill assessment of the regional ocean modeling system” by Haidvogel et al. *J. Comp. Phys*. 227: 3595–3624. *Journal of Computational Physics*. 228(24): 8985–9000.
- Sheinbaum J, et al. 2002. Flow structure and transport in the Yucatan Channel. *Geophys Res Lett*. 29(3):10–1–10–4.
- Skamarock WC, et al. 2005. A Description of the Advanced Research WRF Version 2. NCAR Technical Note, NCAR/TN-468+STR.
- Sturges W, Leben R. 2000. Frequency of ring separations from the loop current in the Gulf of Mexico: A revised estimate. *J Phys Ocean*. 30(7):1814–1819.
- Taylor KE. 2001. Summarizing multiple aspects of model performance in a single diagram. *J Geophys Res*. 106(D7):7183–7192.
- Tolman H. 2002. User manual and system documentation of WAVEWATCH-III version 2.22. US Department of Commerce, NOAA.
- Vukovich FM, et al. 1979. Some aspects of the oceanography of the Gulf of Mexico using satellite and in situ data. *J Geophys Res*. 84(C12):7749–7768.
- Warner JC, et al. 2008. Development of a three-dimensional, regional, coupled wave, current, and sediment-transport model. *Comput Geosci*. 34(10):1284–1306.
- Warner JC, et al. 2010. Development of a coupled Ocean-atmosphere-wave-sediment transport (COAWST) modeling system. *Ocean Model*. 35(3):230–244.
- Xue Z, et al. 2013. Modeling ocean circulation and biogeochemical variability in the Gulf of Mexico. *Biogeosciences*. 10(11):7219–7234.
- Zambon J, He R, Warner JC. Prediction of Hurricane Ivan using a Coupled Ocean-Atmosphere-Wave-Sediment Transport (COAWST) Modeling System. *Weather and Forecasting* (in revision).